
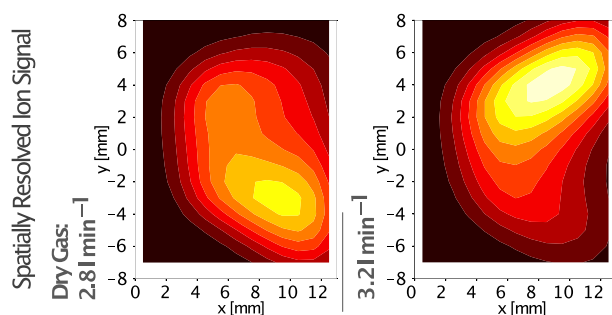


Systematic Ion Source Parameter Assessment by Automated Determination of the Distribution of Ion Acceptance (DIA) Using APLI

Walter Wißdorf,¹  Matthias Lorenz,^{1,2} Klaus Brockmann,¹ Thorsten Benter¹

¹Department of Physical and Theoretical Chemistry, University of Wuppertal, Gauss Str. 20, 42119, Wuppertal, Germany

²Present Address: Oak Ridge National Laboratory, Center for Nanophase Materials Sciences, 1 Bethel Valley Rd, Oak Ridge, TN 37831-6493, USA



Abstract. The determination of the spatially resolved ion signal with atmospheric pressure laser ionization (APLI), which was introduced as distribution of ion acceptance (DIA), serves as a valuable tool for the understanding of complex and highly dynamical conditions in modern atmospheric pressure (AP) ion sources. DIA provides information about fluid dynamics, ion transport, and ion transformation processes in such sources and is an ideal basis for the validation of numerical

models of the dynamics in the ion source enclosure.

Keywords: Atmospheric pressure ionization, API, Ion sources, Laser ionization, APLI, Spatially resolved ionization, Ion source parameters, Gas flows

Received: 27 December 2017/Revised: 20 February 2019/Accepted: 25 February 2019/Published Online: 8 May 2019

Introduction

Over the past decades, technological achievements enabled the application of mass spectrometry and allied techniques to nearly all fields of chemical, biological, and medical analysis. Today, mass spectrometry in combination with atmospheric pressure ionization (API) is one of the most important analytical techniques [1]. However, the understanding and optimization of atmospheric pressure ion sources remain a challenge, and the common knowledge about defined operational parameters in such sources is rather poor. This is primarily due to the high complexity of the conditions in such devices: the high background gas pressure translates to a high collision frequency between generated ions and bulk gas molecules. This has profound consequences: the trajectories of ions in AP ion sources depend not only on the prevailing electrical

fields but also to a large extent on the generally complex fluid dynamics of the bulk gas [2, 3]. Further, the high collision frequency potentially leads to bi- and termolecular chemical reactions between ions and background components at the collision rate limit or even above [4]. The walls of the ion source chamber are also affected by the high gas pressure: in stark difference to the conditions in classical low pressure ion sources, metal and glass surfaces in typical AP ion sources are covered with molecular layers of solvents and bulk gas components, predominantly with water [5, 6]. Therefore, surface reactions potentially also affect the performance of API-MS instruments.

Due to this level of complexity, systematic experimental and theoretical investigations are required to gain deeper insight into the physical and chemical conditions in AP ion sources, to identify critical operational parameters, and ultimately to design new sources with improved performance. One approach to generate useful experimental information, which can be utilized for the validation of numerical models, is the measurement of the spatially resolved ion signal, the *distribution of ion acceptance (DIA)* [7, 8]. DIA measurements are ideally acquired with atmospheric pressure laser ionization

Electronic supplementary material The online version of this article (<https://doi.org/10.1007/s13361-019-02190-x>) contains supplementary material, which is available to authorized users.

Correspondence to: Walter Wißdorf; e-mail: wissdorf@uni-wuppertal.de

(APLI) [9]. In past publications and conference contributions, we have demonstrated the applicability of DIA measurements to general questions regarding the chemical dynamics in API sources [10–12], ion transport in an API source [13], and the analytical optimization of a source design [14]. Furthermore, experimentally determined DIA datasets were used to validate numerical simulations of the fluid dynamics in an API source [2] and trajectory simulations of ions [3, 15].

There are other spatially resolved visualization methods, which are complementary to DIA measurements: methods as laser-induced fluorescence (LIF) are able to determine the concentration distribution of an appropriate neutral analyte [16, 17]. More sophisticated experimental setups allow to determine solvation states or protonation states of analytes in spray droplets [18, 19]. Particle image velocimetry [2, 20] or Schlieren techniques [21–24] are methods to gather information about the neutral gas dynamics (e.g., the flow and temperature field) in an AP ion source. All those methods can contribute to a comprehensive picture of the complex processes in an AP ion source. However, to the best of our knowledge, DIA measurements are the only method able to determine the effective spatially resolved ion signal.

The combination of experimental DIA and numerical results gave a much deeper insight into the dynamics of the investigated commercial Bruker multipurpose ion source (MPIS) [25].

The experimental part of these elaborate investigations is presented in this contribution. Fully automated DIA measurements were used to perform wide-range variations of several ion source settings, which in turn allowed the identification of critical operational parameters. With this setup, over 700 individual DIA measurements were acquired. This paper presents an overview of the automated measurement setup and some highlighted results along with conclusions concerning the influence of ion source parameters on the DIA.

Methods

Experimental Setup

DIA were measured in a commercial AP ion source (Bruker Multi Purpose Ion Source, Bruker Daltonics, Bremen, Germany), attached to an orthogonal TOF-MS (Bruker micrOTOF, Bruker Daltonics, Bremen, Germany). Figure 1 shows an overview of the experimental setup. An analyte solution was sprayed into the ion source chamber and the desolvated analyte was ionized in the target volume (g in Figure 1) by spatially resolved two-photon laser ionization (atmospheric pressure laser ionization, APLI) [1, 9, 26]. The resulting ions were subsequently sampled and mass-analyzed by the TOF-MS.

A 248-nm KrF* Excimer Laser (Atlex 300 SI, ATL Lasertechnik, Wermelskirchen, Germany) was used as laser light source. The laser beam was shaped by a circular aperture with a diameter of 5 mm and directed through a fused silica lens with a focal length of 125 mm. This lens was mounted on a custom positioning stage, which allowed movement on a plane perpendicular to the laser beam axis as indicated in Figure 1.

With the moving lens, the focal point of the laser beam moves accordingly. This setup allowed to scan the source volume with the laser beam and to measure a spatially resolved ion signal in terms of recorded ion intensity (which is the combined result of ion generation, ion transmission to the MS inlet, and potentially ion chemistry) in dependence on the ionization position. As indicated in the lower panel of Figure 1, this setup induces a slight perspective distortion because the ionizing beam is mostly not exactly parallel to the z -axis. In addition, with the present setup, it is not possible to resolve the ionization volume in z -direction. This is due to the generation of ions even in the unfocused beam. An intensity reduction to the extent that two-photon ionization is only occurring within the beam waist around the focus is essentially not possible with the present setup. Thus, two dimensional *projections* of the in fact three-dimensional DIA are measured.

The principle of operation to measure spatially resolved ion signals has been published [7], along with detailed information on the perspective distortion, the light intensity profile along the laser beam travel path, and the lens positioning stage.

Ion Source/Ion Source Parameters

The MPIS is composed of an aluminum chamber, which is attached to the front end of the inlet system of the TOF-MS. The ion source was used in LC configuration: an analyte solution (2 in Figure 1) was pumped into the heated nebulizer (f in Figure 1) where it was pneumatically sprayed with an additional *nebulizer gas* flow (1 in Figure 1). The vaporized and desolvated analyte (4 in Figure 1) was ionized in the target volume (g in Figure 1) in the main chamber of the ion source by the laser radiation. A second heated gas flow, the *dry gas* (3 in Figure 1), counters the nebulizer gas flow. Its purpose is to support the evaporation of solvent droplets and to keep the MS inlet (d and e in Figure 1) free of remaining solvent droplets.

Ions are sampled by the MS, if they reach the entrance of the inlet capillary (c in Figure 1) from where they are transported into the MS inlet stage by the rapid gas flow through the inlet capillary duct. Since the dry gas constantly flushes the region between inlet capillary and the outermost ion optical element of the MS inlet stage, termed “spray-shield” in Bruker instruments (e in Figure 1), the ions have to be electrically attracted towards the MS inlet. For this purpose, the spray-shield and a metallic cap on the capillary (d in Figure 1) are imposed with *attractive* electric potentials. In combination, both elements act as an electrostatic lens, which focuses the ions onto the capillary entry. Due to the operation of the MS in positive ion mode, all potentials presented here are *negative* with respect to ground potential if not noted otherwise. The voltage on the capillary cap is typically in the range of 1–3 kV with APLI operation; the potential on the spray-shield is generally much lower. Common voltages are in the range of 50–500 V in this case. Due to the observation that the internal power supply of the MS for the spray-shield was not reliable when operated with voltages at or below 50 V, a programmable external power supply (Votcraft PSP 1803, Conrad Electronic SE, Hirschau, Germany) was used

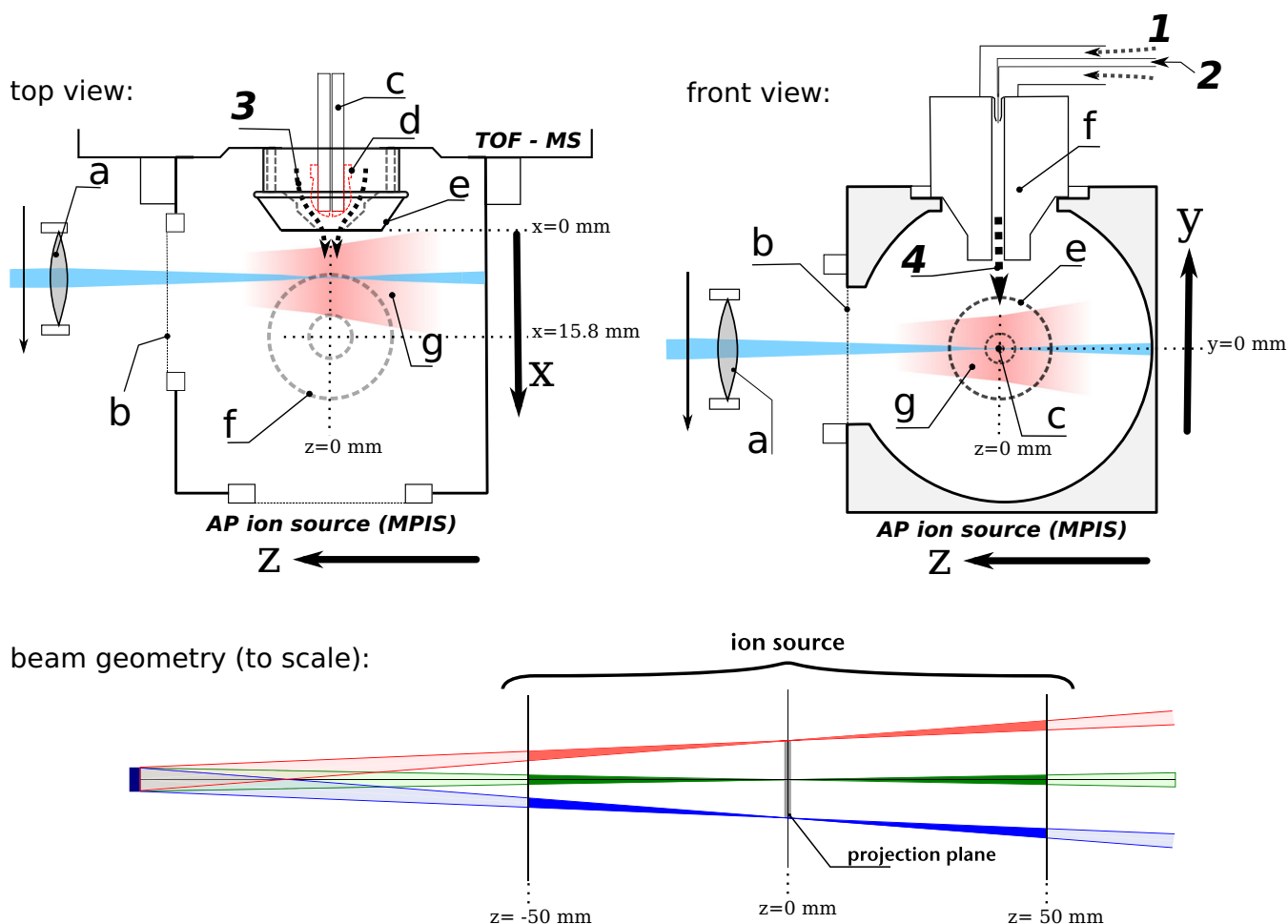


Figure 1. Experimental overview. (a) Movable focusing lens, (b) fused silica window, (c) MS-inlet capillary, (d) MS-inlet capillary cap., (e) spray-shield, (f) nebulizer (default position), (g) ionization zone, 1 nebulizer gas, 2 liquid analyte solution, 3 dry gas, 4 analyte/solvent vapor mixed with nebulizer gas. The lower panel shows the geometry of the ionizing laser beam to scale in frontal view. The blue and red beams are the outer margins of the scan area in y -direction (blue $y = -8$ mm and red $+8$ mm on the projection plane)

as source for the spray-shield voltage. As described in detail in the following, the output voltage of this power supply was remotely adjusted *in reference* to the spray-shield voltage by the MS software. This custom operation of the external power supply allowed to adjust the critical spray-shield voltage in automatized measurements.

The flows and temperatures of the dry and nebulizer gas were also remotely controlled in automatized DIA measurements. Both gas flows were controlled by the internal flow controller system of the MS. The dry gas flow is directly configured as a volume flow in the MS control software. An additional flow meter (500 L h^{-1} Rotameter, Krohne Messtechnik GmbH & Co, Duisburg, Germany) independently monitored the absolute dry gas flow. The dry gas was heated by the dry gas heater, which is integrated into the ion source interface of the MS. The temperature was monitored and controlled by the MS.

The nebulizer gas flow is adjusted by the MS control software by means of a gas overpressure with respect to ambient pressure. To correlate the nebulizer gas pressure with a gas volume flow and to monitor the internal gas supply system, an

additional mass flow meter (FM-360, Tylan Corporation) was mounted between the internal flow controller and the nebulizer. The nebulizer gas was heated by the nebulizer block. Similarly to the dry gas, the nebulizer heater temperature was monitored and controlled by the MS.

In addition to the described parameters of the ion source, which were adjustable in automatized measurements (voltages, gas flows, and temperatures), the nebulizer position was manually adjustable by about 13 mm on the x -axis. In its default position, the nebulizer has the greatest possible distance to the MS inlet, which was independently shown to be favorable for analytical APLI operation. In this case, the nebulizer inlet nozzle, which is defined as the central axis of the nebulizer, has a distance of 18 mm to the front face of the spray-shield.

For the dry and nebulizer gas supply, nitrogen with 99.999% purity from compressed gas cylinders (Messer Group GmbH, Sulzbach, Germany) was used. Pyrene served as APLI analyte (purity and origin unknown). Stock solutions were prepared in HPLC grade methanol or pentane, respectively. The concentration of the solutions used in the automatized DIA measurements prepared from the stock solutions was $1 \mu\text{mol/L}$.

The analyte solutions were injected into the LC sprayer/heater of the MS by an HPLC pump (Model L-7110, Hitachi Ltd., Tokyo, Japan) with a liquid flow rate of 100 $\mu\text{L}/\text{min}$. Also, a manual set of experiments was conducted with benzo[a]pyrene, toluene, and nicotine solved in acetonitrile. Here, the concentrations and liquid flow rates differed. The parameters are noted separately the section “Chemical Effects”.

Measurement Automation

As already stated, the measurement setup allowed fully automated DIA measurements. Figure 2 schematically depicts the elements of this automation setup and the corresponding control flow. Central to the entire setup is the TOF-MS, which is controlled by a personal computer over a serial data connection. The time of flight measurement is also performed in this computer by a dedicated digital transient recorder card (digitizer). Critical for the DIA measurement automation was the ability of the MS control software (Bruker MS control version 2.2) to define multiple segments with individual ion source configurations in a chromatographic run, which we used to set up DIA measurements as individual segments. The optical scan in a DIA measurement is defined by a “scan program”, which consists of a list of spatial positions and their individual dwell times. The scan programs are defined in “scan files”, which are interpreted by a custom optics control program running on a second personal computer, which is directly connected to the lens stage. In the case of the MPIS, the scan programs are essentially rectangular grids with identical integration times for all spatial positions. Typical integration times per spatial position were in the range of 2–10 s, spatial resolutions were 1×1 mm (13×16 grid points) or 0.5×0.5 mm (27×33 grid points) in the x - and y -direction, respectively.

As described in detail in a previous publication [7], the reference between spatial position and recorded signal intensity

is the passed time since scan start, which is the start time of the individual segment in the automated measurements.

To control the external power supply for the spray-shield voltage, the control channel between control computer and MS was monitored with a dedicated custom program. This program translated the “voltage set commands” for the MS into according commands for the external power supply.

In standard operation, the measurement segments are defined by the MS user in the graphical interface of the MS control software. The MS control software saves the definition of the measurement segments in “method files”, which are XML files generated by the Bruker MS software. The manual configuration of the measurement segments is potentially error-prone in the generation of comparably long and complex segment definitions in systematic DIA measurements. To avoid such errors, a further custom program generated valid XML method files from a tabular definition of the planned DIA measurement series, which were then used as input for the MS control software.

To ensure the stability of the entire measurement system as well as the ion source, a standard DIA segment was measured at the beginning and at the end of a measurement series. In long-term measurement programs, additional test segments in the measurement series were performed.

Data Analysis

Figure 2 schematically depicts the data analysis procedure leading to DIA results: The Bruker Data Analysis program reads the recorded MS raw data of the measurement series and generates mass traces for m/z ratios of interest. Since the radical cation (M^+) is essentially the single analyte signal under APLI conditions, we exported the mass trace for $m/z = 202$ and the total ion current (TIC) for comparison and validity control to text files. A custom Python program then calculated the two-

Control Flow:

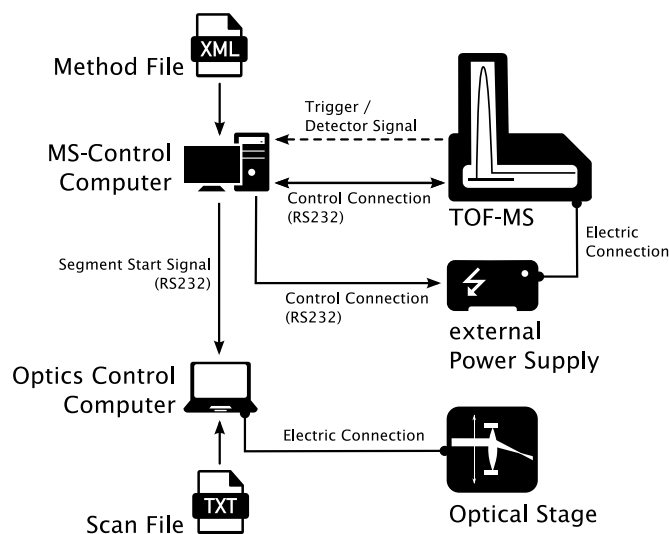
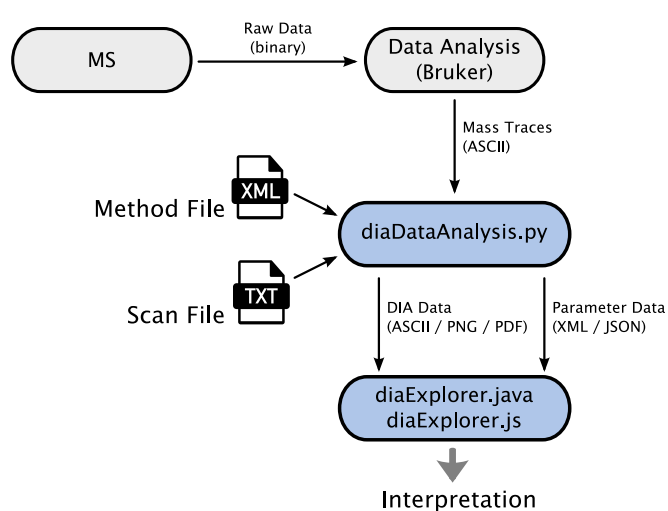


Figure 2. Experiment control- and data-flow

Data Flow:



dimensional DIA results for the two extracted ion signals from the mass traces and the scan files. The results were exported for further processing and rendered as two-dimensional contour plots. In addition, the Python program generated meta-data files (in XML and JSON format), which contain the configuration and calculated statistical information (e.g., mean and maximum signal intensity) for the individual DIA measurements.

To efficiently elucidate the resulting large multidimensional data set, two custom data analysis tools were developed, which we refer to as “DIA explorer”. The first one was implemented in the Java and Groovy programming languages. It allows to view and efficiently filter the large set of DIA measurements on a freely configurable two-dimensional “bubble-plot”. A second, simplified version was implemented as browser-based web application, which allows to interactively present DIA measurements to, e.g., an audience. We published the online version of the DIA explorer with simulated and experimental data sets at <http://dia.ipams.uni-wuppertal.de>.

Numerical Simulation

We have systematically simulated the DIA in a numerical model using SIMION [27] in combination with the statistical diffusion simulation (SDS) algorithm [28, 29]. Details about the implementation of the DIA model and the results can be found in a previous publication [3] and in conference contributions [15, 30]; therefore, the numerical model is only briefly discussed.

The basis for these simulations was an experimentally validated computational fluid dynamics (CFD) model of the gas dynamics in the ion source, performed by Pöhler et al. [2]. The resulting fields (velocity, temperature and pressure fields, distribution of the neutral analyte) were used as input parameters for ion trajectory simulations in SIMION/SDS. Individual “packages” of ions were started from positions on a spatial grid similar to the measurement grid of the DIA measurements. The termination positions of the simulated ions were recorded. The simulated DIA was calculated by counting the number of ions terminating in a predefined target zone corresponding to the entrance of the inlet capillary. To simulate the effects of ion depletion reactions, we simply assumed a first-order ion depletion reaction, which was considered in the numerical model using an adapted version of the Reaction Simulation (RS) extension [31] for SIMION/SDS.

Results and Discussion

In the following, we use the term dynamic ion acceptance volume (DIAV) as defined in [7] as the volume with a signal intensity, which is at least 1/e of the maximum intensity in the DIA. With this definition, this volume corresponds well to the volume, which is intuitively considered as spatially resolved intensity.

The origin of the coordinate system ($x=0$, $y=0$) in the presented DIA plots corresponds to the intersection between

the front plane of the spray-shield and the main axis of the inlet capillary, which we defined as the x -axis of the ion source.

Overview and General Ion Source Parameter Effects

Owing to the fully automated measurement procedure, over 700 DIA measurements were performed within 14 weeks. The parameter space of the considered ion source settings was systematically probed. The ranges of the individual settings and the default operational point, which was also used as standard DIA segment for the stability verification (with only the manually adjustable nebulizer position as exception), are presented in Table 1.

Effects of Electric Potentials

Figure 3 depicts the effects of variations of the electric potentials in the ion source. The general shape of the DIAV shown in Figure 3 is typical for the obtained DIA results: commonly, a bimodal distribution is obtained, with a significant local signal minimum slightly above the center axis of the ion source ($y \approx 1.5$ mm). This structure is located in some distance to the MS inlet; in direct proximity to the spray-shield, a nearly complete signal loss is observable. With increasing capillary voltage, the whole structure is moved further away from the MS inlet, but the general shape of the DIAV is not significantly affected despite a partial overall signal decline. In particular, the inclination angles on the MS facing side of the DIAV (left on the DIA plots) remain rather unaffected when the capillary voltage is increased.

An increase of the spray-shield voltage also shifts the DIAV away from the MS inlet. In contrast to the potential on the capillary cap, the absolute voltage on the spray-shield, which has a significant effect on the DIAV, is much lower. The detailed analysis of the electrical field structure in the ion source provides a rationale for this observation: the capillary-cap potential has to reach through the comparably small orifice in the spray-shield. Therefore, the spray-shield also effectively “shields” the field induced by the capillary cap, while the field from the spray-shield itself can penetrate the ion source volume without restriction. In addition to the much higher sensitivity of the DIAV on the spray-shield potential, its shape is much more altered by the spray-shield voltage: the DIAV is compressed on the y -axis and the inclination becomes significantly lower, while a simultaneous shift away from the MS inlet occurs. In addition, the observed signal intensity drops significantly, which can be due to the fact that the maxima of the DIAV leave the scanned spatial region with increasing spray-shield voltages. The described general effects of the variable electric potentials in the ion source were observed for all DIAs with the nebulizer set in its default position (18 mm).

Effects of Gas Flows and Operational Switch Point

The default configuration of the dry gas for analytical APLI operation is 3.0 L/min at a temperature of 200 °C with the

Table 1. Ion Source Parameter Space and Default DIA Segment

Parameter	Range	Default
Voltage on capillary-cap (negative to ground)	100–4000 V	1000 V
Voltage on spray-shield (negative to ground)	0–1000 V	0 V
Dry gas flow	0.6–5.0 L/min	3.0 L/min
Nebulizer gas pressure	0.2–4.0 bar	3.0 bar
Dry gas temperature	50–300 °C	200 °C
Nebulizer gas temperature	20–325 °C	320 °C
Nebulizer position	5–18 mm	18 mm

nebulizer in its default position. The variation of the dry gas around this operational point, as presented in Figure 4, reveals that the effect of the dry gas on the DIAV differs significantly from the effect of the electric potentials: despite the increased counter gas flow, which has to be traversed by the ions, the DIAV is not shifted away from the MS inlet and the position of the signal maximum and the DIAV margins on the x -axis remain stable. However, there is a distinct and rather abrupt “switching” of the DIAV from a distribution with a signal maximum below the central axis of the ion source (0 on the y -axis) to a distribution with a global signal maximum above this axis. This phenomenon is clearly observed in the first row (50 °C) of Figure 4. Supplemental Figure 1 shows the transition between the two states in more detail. The figure shows that the transition takes place over a dry gas increase of 0.3 L/min while the DIAV remains stable after the transition has occurred. Such an abrupt switching between two clearly discernable states of the DIAV in dependence on the gas flows was never observed elsewhere in the investigated parameter space.

The position of the DIAV switching in the parameter space spanned by the dry gas flow and temperature, respectively, clearly depends also on the latter: as seen in Figure 4 and in greater detail in supplemental Figure 1, the DIAV transition shifts towards higher dry gas flows with increasing dry gas temperature: at 50 °C, the signal maximum has transitioned to positive x -coordinates at 3.0 L/min. At 150 °C, a similar stage of the transition is reached at 3.2 L/min while at 250 °C, the signal maximum has not yet shifted above the central axis of the ion source at this dry gas flow.

The effects of a variation of the nebulizer gas parameters are depicted in Figure 5 and supplemental Figure 2. They are generally comparable to the effects of the dry gas variation: the DIAV is not shifted entirely on the x -axis, instead a similar transition of the signal center from a position below the central axis towards the top of the ion source as discussed for the dry gas is observable, as shown in Figure 5: The distribution extends upwards with increasing nebulizer pressure while it moves downwards with increasing nebulizer temperature. In contrast to the abrupt signal shift in dependence on the dry gas flow, with regard to the nebulizer gas flow, the transition region is much broader. Supplemental Figure 2 shows that for, e.g., 20 °C nebulizer temperature, the shift towards the upper region of the scanned area occurs over a nebulizer-pressure range of at least 3 bar. This corresponds to a flow increase of approximately 1.5 L/min as compared to 0.4 L/min for the dry gas. In

addition, the overall signal intensity is apparently highest in the transition, when the DIAV is near to symmetrical around the central axis of the ion source.

The combined results of the dry and nebulizer gas variation suggest that the signal shift on the y -axis is probably the result of changes in the ion transport and neutral analyte distribution due to a changed structure of the bulk gas flow in the ion source.

The performed CFD [2] and ion trajectory simulations support this notion. Figure 6 and supplemental Figure 3 show exemplary DIA simulations in comparison to the performed DIA measurements. As presented in reference [3] and also discernible in the comparisons here, the simulation does not entirely reproduce the distinct and abrupt signal shift observed in the DIA measurements. Instead, the simulations reproduce particular aspects of the experimental results, e.g., the position of the signal maximum for 2.0 L/min dry gas and the general inclination angles of the DIAV (cf. Figure 6). With increasing dry gas flow, the simulated DIAV tends to shift upward in most of the performed simulations (supplemental Figure 6 shows also a counterexample with the results for 0 V spray-shield voltage). Since only two dry gas configurations were available from the CFD simulation of the MPIS, it remains currently unclear whether the simulated DIAV fully transitions to a state similar to the experimentally observed. A critical analysis of the calculated ion trajectories revealed that the spatial resolution of the CFD and ion trajectory simulations is probably too low to fully reproduce the experimentally observed “switching” of the DIAV. Particularly, the area in close vicinity to the MS capillary inlet and the inflow into the inlet capillary has to be resolved with very high accuracy, since the simulated DIA is highly sensitive to the exact location, size, and shape of the target zone, where terminating ions are counted as contributing to the simulated DIAV. The obtained experience with the dynamics of the ion trajectories within the MPIS is the base for new, more refined simulation efforts of such ion sources.

Effects of Nebulizer Position

The manual variation of the nebulizer position has a profound effect on the measured DIA, which is clearly seen in Figure 7. The DIAV shape changes significantly with the shift of the nebulizer towards the MS inlet (e.g., for a decreasing nebulizer position value as used in Figure 7): a new signal maximum occurs in the upper half of the scanned area, which correlates

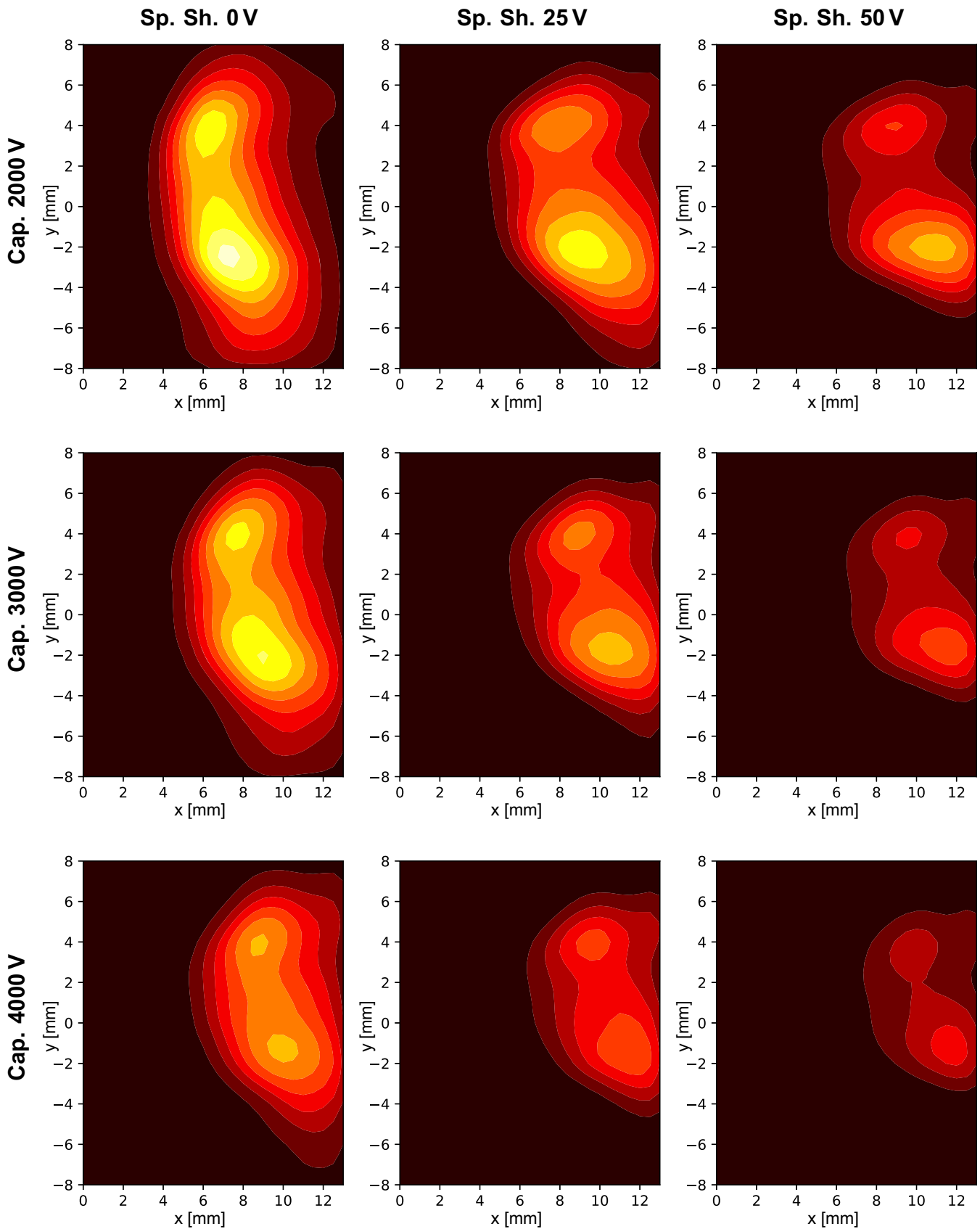


Figure 3. Effects of the capillary (from top to bottom) and spray-shield (from left to right) voltages on the measured DIA. The dry gas flow was 2.0 L/min at a dry gas temperature of 200 °C, the nebulizer gas pressure was 3.0 bar at a nebulizer temperature of 320 °C, the nebulizer was in its default position (18 mm). The maximum signal intensity (brightest contour) is 35,000 counts

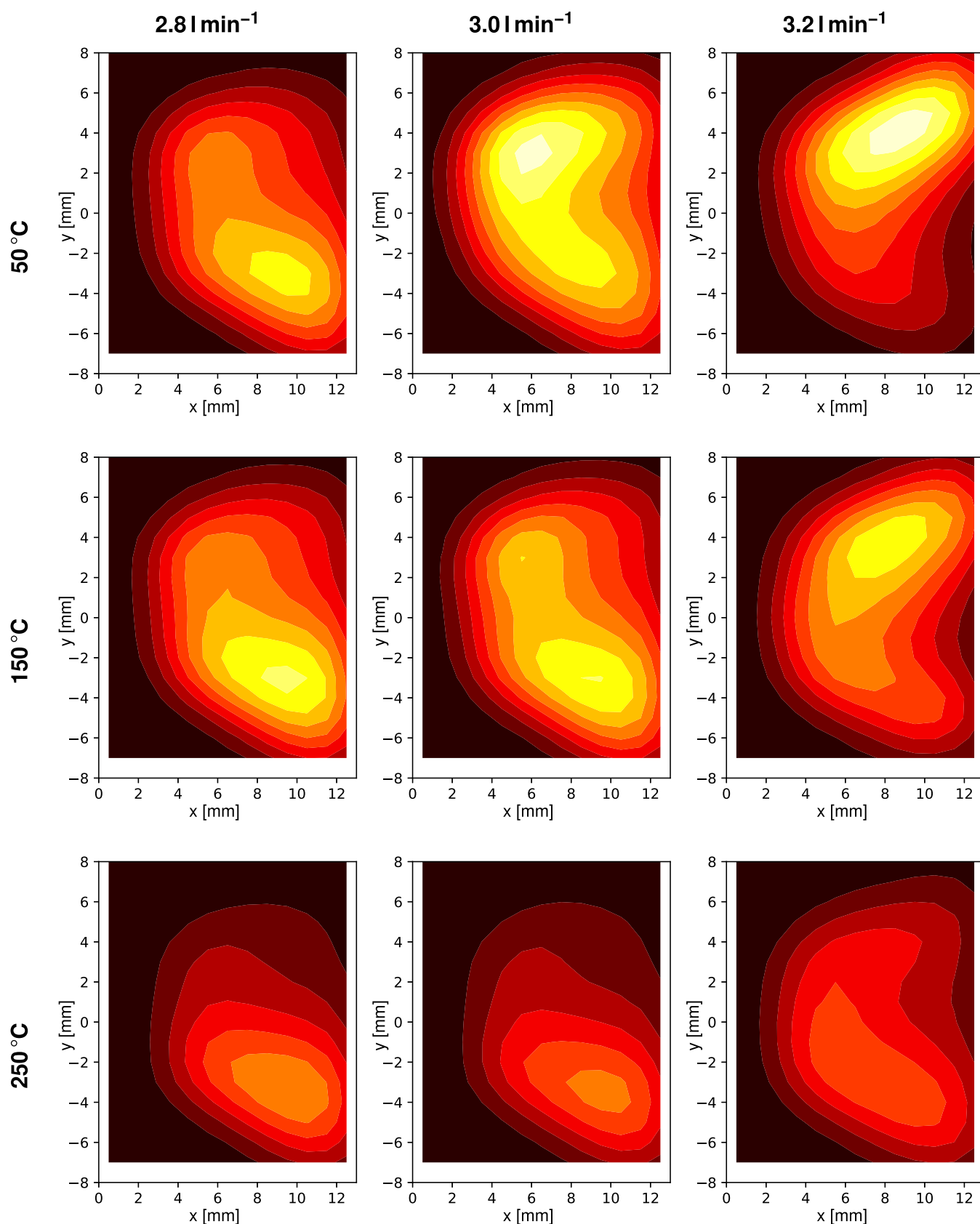


Figure 4. Effects of the dry gas flow (from left to right) and temperature (from top to bottom) on the measured DIA. The capillary voltage was 1000 V, the spray-shield voltage was 50 V, the nebulizer gas pressure was 3.0 bar at a nebulizer temperature of 325 °C, the nebulizer was in its default position (18 mm). The maximum signal intensity (brightest contour) is 175,000 counts

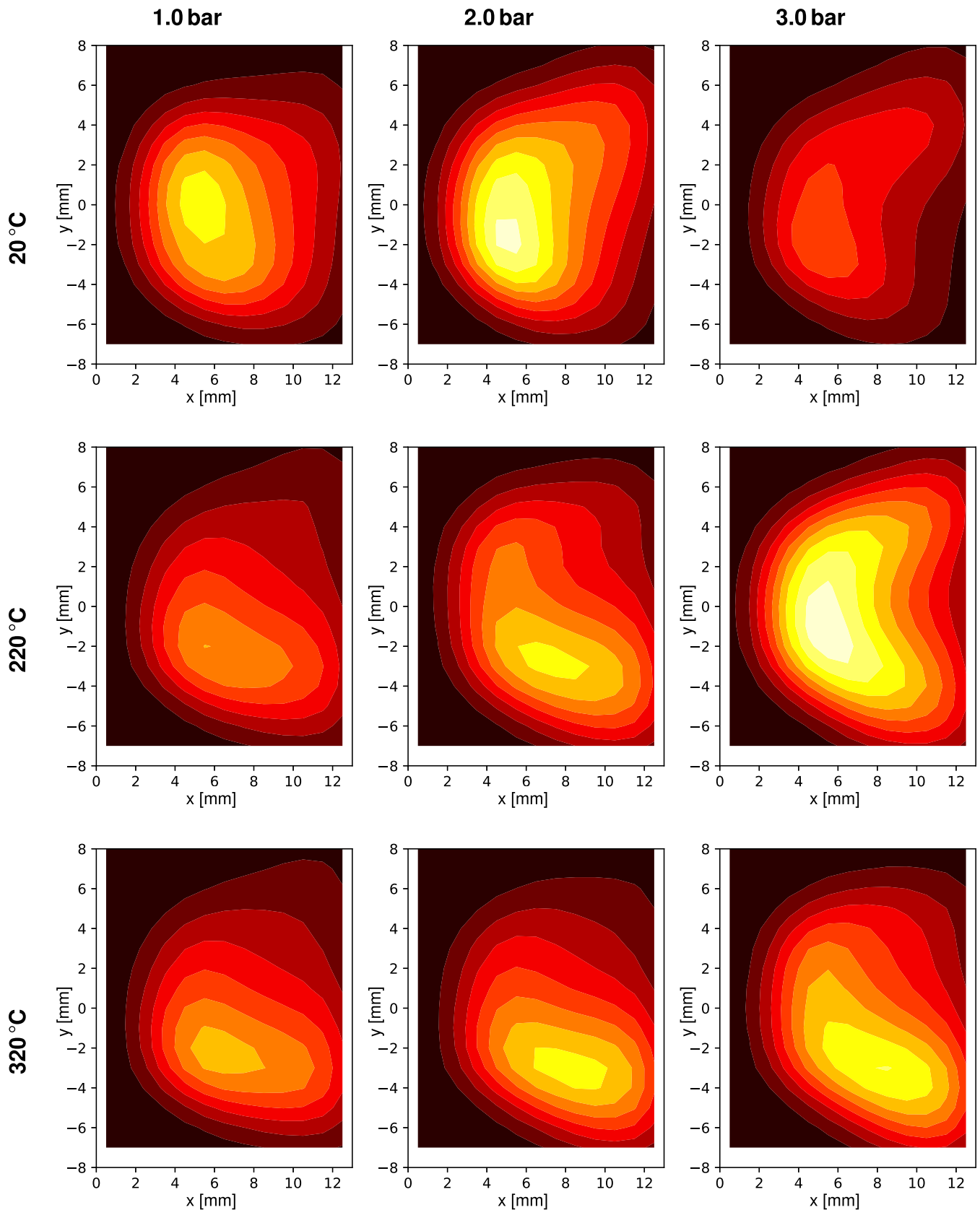


Figure 5. Effects of the nebulizer gas flow (from left to right) and temperature (from top to bottom) on the measured DIA. The capillary voltage was 1000 V, the spray-shield voltage was 50 V, the dry gas flow was 3.0 L/min at dry gas temperature of 200 °C, the nebulizer was in its default position (18 mm). The maximum signal intensity (brightest contour) is 140,000 counts

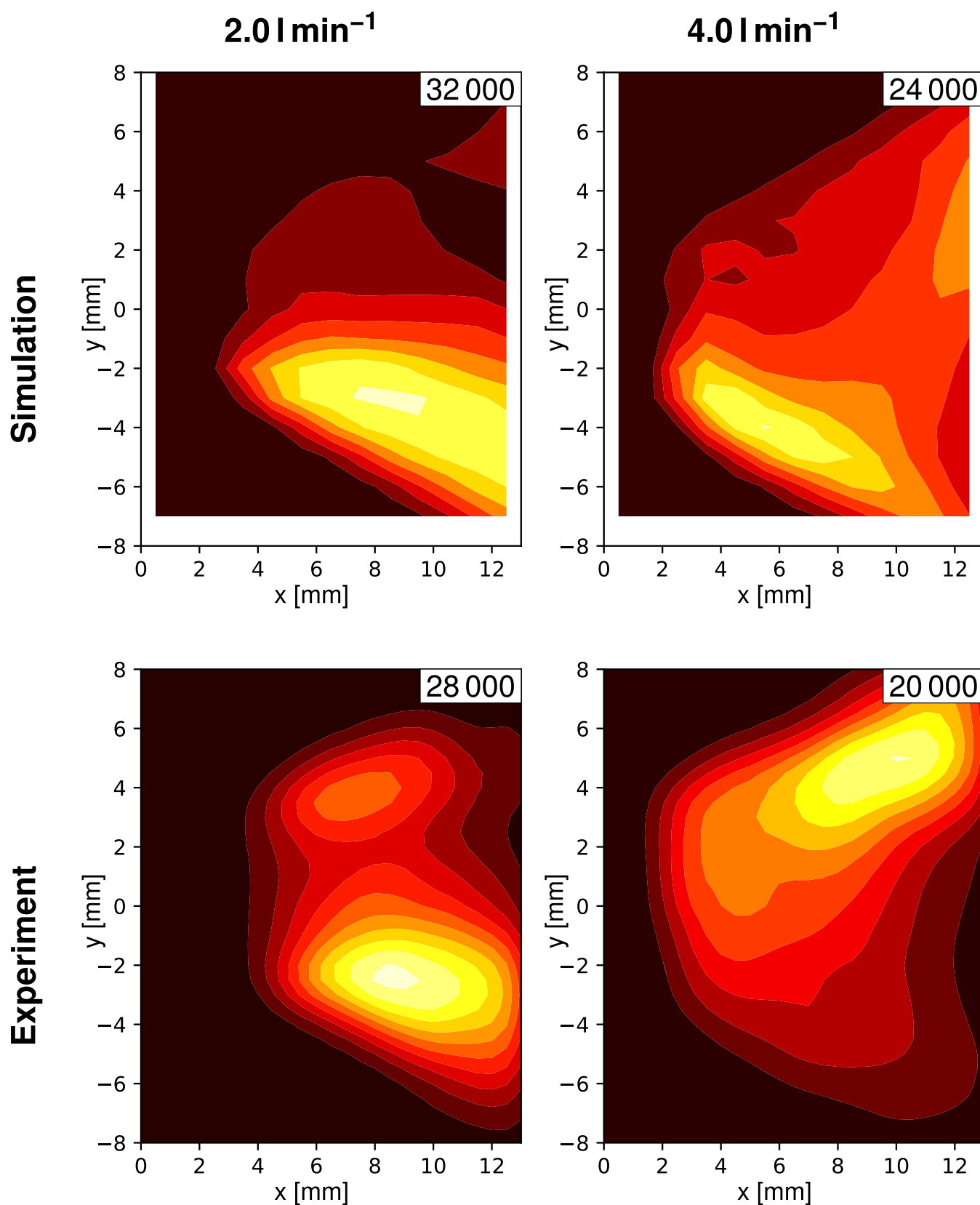


Figure 6. Measured and simulated transition of the DIAV in dependence of the dry gas flow: the capillary voltage was 1000 V, the spray-shield voltage was 50 V, the nebulizer pressure was 3.0 bar at a temperature of 320 °C, the dry gas temperature was 200 °C. The maximum signal intensity (brightest contour) is given in the insets

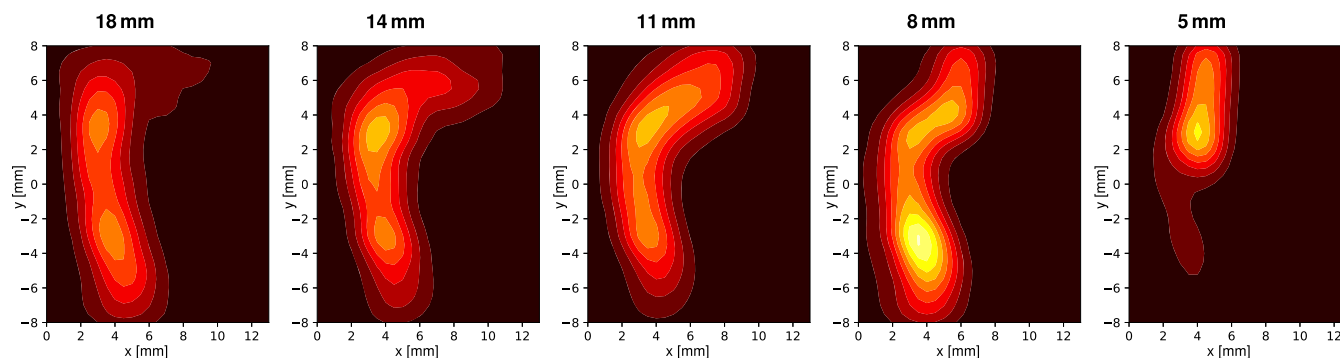


Figure 7. Effects of the variation of the nebulizer position on the measured DIA. The capillary voltage was 1000 V, the spray-shield voltage was 0 V, the dry gas flow was 3.0 L/min at 200 °C, the nebulizer pressure was 3.0 bar at 320 °C. The default position of the nebulizer is 18 mm. The maximum signal intensity (brightest contour) is 64,000 counts

with the nebulizer position, i.e., it moves towards the MS inlet with the nebulizer. Finally, only a confined signal maximum remains, which is located in front of the nebulizer. This signal distribution is very stable in this state, which is shown in the supplemental Figures 4.1 to 4.3. Particularly, with a reduced dry gas flow, which is depicted in supplemental Figures 4.2 and 4.3, the signal is almost unaffected even by considerable variations of the capillary and spray-shield voltages. In contrast to the situation with the nebulizer in its default (completely retracted, 18 mm) position, neither the position nor the shape of the DIAV is sensitive to changes of the electrical potentials in the ion source and even the absolute signal intensity is mostly unaffected.

The supplemental figures also demonstrate (cf. e.g., the results with a capillary voltage of 4000 V shown in supplemental Figure 4.3) that the position of the additional signal maximum directly correlates with the position of the nebulizer: the additional signal is reproducibly located approximately 1.5 mm closer to the MS inlet with respect to the nebulizer position (lower x -values in supplemental Figure 4.3).

The sum of these findings strongly suggests that the changes in the DIA shapes are the results of the changes of the bulk gas flow dynamics inevitably induced by the modification of the nebulizer position. A changed flow pattern changes the trajectories of ions in the bulk gas flow due to the viscous interaction between bulk gas and ions. In addition, changes of the bulk gas flow change the distribution of the neutral analyte. Which of the two effects is the primary reason for the observed changes in the DIA cannot be concluded from the current experiments. Numerical DIA simulations would readily answer this question, but to date, there is no CFD model for the MPIS with a modified nebulizer position available. Nevertheless, the DIA measurements obviously visualize an effect of a change in the fluid dynamics in the ion source, which underlines the applicability for the validation of numerical models.

Supplemental Figure 4.1 shows also an unexpected dependence of the DIAV on the spray-shield voltage: there is a reproducible discontinuity of the DIAV change with increasing spray-shield potential. In particular with the almost fully retracted nebulizer (18, 14, and 11 mm, cf. supplemental

Figure 4.1), the DIAV initially moves away between 0 and 20 V spray-shield potential, but travels back towards the MS inlet at 25 V. Finally, it moves away again and shifts towards the upper half of the scanned area at 50 V spray-shield potential. This particular effect was not reproduced in the numerical DIA simulations. There are no recordings of DIAs with 20 V spray-shield potential for other dry gas flows than 3.0 L/min; thus, it remains unclear whether this effect is also present for different flow conditions in the ion source. The described finding implies though that the response of the DIA on the electrical potentials in the ion source may be much more pronounced than suggested by the presented DIA measurements. Since the DIA measurements for the step-wise changed nebulizer position were performed on different days, a random measurement artifact is excluded as cause for the observed behavior of the DIAV. To investigate the dynamical behavior of the DIA, subsequent experiments in the future are planned, which will resolve the electric parameters in much higher detail. In combination with CFD and ion trajectory simulations for changed nebulizer positions, they will probably complete the understanding of the ion dynamics in the MPIS run in the LC configuration.

Chemical Effects

DIA measurements with a Waters Z-Spray type AP ion source revealed that the spatially resolved ion signal distribution generally depends on chemical parameters as well, e.g., on the chemical identity of the observed ion (radical cation vs. protonated molecule) or on chemical interactions with background components or dopants [7, 10]. Such effects were not observed in the fully automatized DIA measurements using the MPIS; however, investigations regarding the impact of ion chemistry on the DIA were not intended in the present study. Pyrene was selected as analyte in the automatized DIA measurements to deliberately suppress the chemical reactivity of the generated ionic species: pyrene radical cations, which were largely contributing to the total ion signal in the presented automatized DIA measurements, are chemically relatively inert with respect to the matrix constituents (i.e., N_2 , CH_3CN , H_2O), even when present in high mixing ratios.

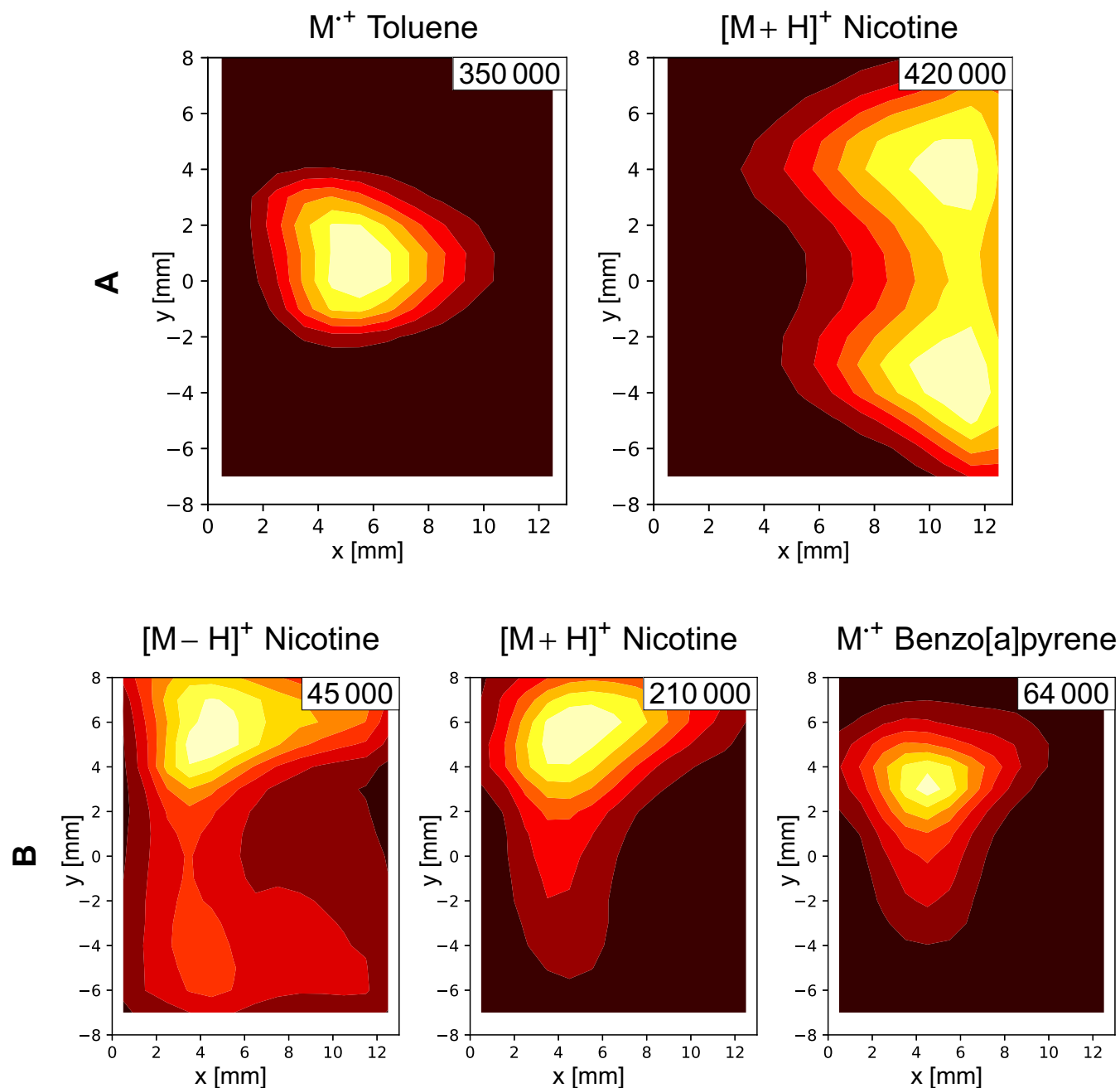


Figure 8. Chemical effects on the DIA in the MPIS. Nebulizer pressure: 3 bar, nebulizer temperature: 325 °C, dry gas temperature: 200 °C, dry gas flow: 3.0 L/min. **(a)** Capillary voltage 1000 V, spray-shield: 0 V, 300 $\mu\text{L}/\text{min}$ of a solution of 0.04 $\mu\text{mol}/\text{L}$ benzo[a]pyrene, 25 $\mu\text{mol}/\text{L}$ nicotine and 9.3 mmol/L toluene in acetonitrile was sprayed. **(b)** Capillary voltage 1000 V, spray-shield voltage: 800 V, 300 $\mu\text{L}/\text{min}$ of a solution of 0.1 $\mu\text{mol}/\text{L}$ benzo[a]pyrene, 2.5 $\mu\text{mol}/\text{L}$ nicotine and 10 mmol/L toluene in acetonitrile was sprayed. The maximum signal intensity (brightest contour) is given in the insets

Nevertheless, we performed preliminary manual DIA measurements with different analytes, solvents, as well as dopants. With more reactive ionic species present in the source region, significantly different DIAVs are observed, which is presented in Figure 8. The lower row (B) shows the DIAVs of the protonated and deprotonated molecules of nicotine, representing species, which are generated by chemical

ionization, versus the radical-cation (M^+) of benzo[a]pyrene (b), which is generated by direct photoionization. All DIAVs significantly differ in position and shape.

The example in the upper row (A) of Figure 8 is even more striking: here, the spatially resolved ion signals of the radical cation of toluene which acts as a dopant when added to the gas phase in large excess over the analyte mixing ratio, and the

protonated molecule of nicotine are essentially mutually exclusive. This finding strongly suggests that the DIA allows to directly visualize effects of the ionization mechanism on the ion distribution. However, in comparison to the results using the Waters API source, the DIA in the Bruker MPIS tends to be far less sensitive to chemical transformations. Even if the presented dependencies (cf. Figure 8) and similar effects (e.g., the dependence of the DIA on the LC solvent) were observed in the MPIS, under most configurations of the ion source, no significant difference between the chemical species occurred. This is most probably caused by the completely different fluid-dynamics and to a lesser extent electric configuration of both ion sources. To investigate such causes in detail, systematic comparative DIA measurements with carefully selected chemical systems need to be performed in both ion sources.

It is noted that the ion chemistry in the main volume of API sources (i.e., in some distance to high-voltage point potentials such as Corona electrodes or ESI needle tips) is in general fully thermodynamically controlled or equilibrated and should be more or less identical in both sources. The ion transfer region, however, will in most cases significantly shift these equilibria and/or induce further ion transformation reactions [32]. The extent of these changes is strongly dependent on the ion transfer optics geometry and settings [33].

Summary and Conclusions

The automatization of the experimental DIA acquisition setup allows to investigate spaces of ion source parameters even with many independent dimensions. This provides a tool to systematically generate large experimental data-sets, e.g., based on methods of multivariate statistics, with complex target functions with relevance to the analytical operation of the ion source with APLI, e.g., the DIAV integral or the DIAV area. Therefore, statistics-driven optimization of the ion source conditions in terms of analytical parameters becomes possible with this setup. Besides the direct application of DIA measurements in the optimization of APLI, they are a potentially valuable tool to investigate the general characteristics and dynamics in AP ion sources operating with other ionization methods also. The spatially resolved ion signal gathered with DIA measurements depends on the convoluted effects of fluid dynamics, the neutral analyte distribution, the migration of the ions in the ion source, and potentially ion chemistry. Therefore, particularly fluid dynamical calculations and ion trajectory simulations can be assessed and validated by comparison with DIA measurements: a full numerical model of an ion source must be able to reproduce a DIA experiment.

The change in the shape and position of the DIAV with changed nebulizer position as well as the significantly different effect of the electric potentials in the ion source on the spatially resolved ion signal strongly suggest that the fluid-dynamical conditions in the ion source are largely changing as well. Therefore, subsequent CFD simulations of the MPIS should consider also the nebulizer position, even if this requires a

comparably elaborate change in the simulated geometry and rebuilding of the numerical mesh of the CFD calculation.

The comparison between ion trajectory simulations and DIA measurements also indicates that the obtained current state of the numerical model of the MPIS is not satisfactory, because the DIA “switch” was not numerically reproduced, even if the simulation tends to change in a similar way as the experimentally observed DIA. Therefore, more simulated dry gas operation points should be obtained from subsequent simulations with the existing MPIS discretization, with the nebulizer in its default position. This would allow to investigate if the simulation reproduces the DIA switch with a “wrong” dry gas flow or if the simulation cannot reproduce the switch at all. If the effect is reproduced numerically, the cause of the obviously “wrong” dry gas flow at the simulated switch point can be investigated.

Preliminary data demonstrate that effects on the DIA, which are induced by chemical reactions between ions and background components, are visible also in the MPIS under selected conditions. In comparison to the Waters Z-Spray ion source studied in earlier publications [7, 10], the effects are generally less distinct but they can become very pronounced also, e.g., with large quantities of a dopant present in the ion source. The chemistry in AP ion sources and the almost inevitable transformation of chemical systems/equilibria in the generally electrically “hot” ion transfer stages of mass spectrometers become potentially very complex. DIA measurements of chemically active systems are one out of multiple complimentary tools, along with more traditional mass-spectrometric experiments and numerical kinetics models to investigate the ionization and reaction mechanisms of analyte molecules. For demanding chemical systems, such DIA experiments would not be performed in a common commercial ion source but rather in special purpose devices under preferably very clean and controlled electrical, fluid dynamical, and chemical conditions.

Automated DIA measurements also allow the assessment of the ion source operation conditions in terms of the analytical performance of the MPIS. First, the assessment of the large library of available DIA results shows that the response of the spatially resolved ion signal on the ion source parameters is generally nonlinear and deeply folded. In particular, the DIAV position, area, and integral depend in a complex way on the variable parameters of the ion source. This again underlines the necessity for systematic optimization techniques for the fundamental analytical characterization of modern complex AP ion sources.

The complexity of the overall dynamics in AP ion sources increases when ionization techniques such as ESI or APCI are used. This is due to even more variable parameters (e.g., additional electric potentials or spray parameters as the composition of the sprayed liquid phase) and significantly more complex physical and chemical processes in such sources (e.g., complex multiphase flow, evaporation of spray droplets). Nevertheless, there is no fundamental hindrance for laser-based spatially resolved ion signal measurements under such conditions using, e.g., tracer analytes. It was shown experimentally

[34] that radical cations of polycyclic aromatic hydrocarbons selectively generated in ESI plumes with APLI survive the passage to the analyzer. Such experiments would most probably reveal further insights into the dynamics of these ionization methods as well.

DIA measurements are certainly a specialized tool accompanied with a significant experimental effort. Therefore, they are generally not used for routine operation, but their huge potential in fundamental and applied research makes the necessary effort generally worthwhile.

Acknowledgements

The authors thank Bruker Daltonik GmbH, Bremen, Germany, for long term financial and technical support.

Financial support was given by the German Research Foundation (DFG project BE BE2124/6-1).

References

- Covey, T.R., Thomson, B.A., Schneider, B.B.: Atmospheric pressure ion sources. *Mass Spectrom. Rev.* **28**, 870–897 (2009)
- Poehler, T., Kunte, R., Hoenen, H., Jeschke, P., Wissdorf, W., Brockmann, K.J., Benter, T.: Numerical simulation and experimental validation of the three-dimensional flow field and relative analyte concentration distribution in an atmospheric pressure ion source. *J. Am. Soc. Mass Spectrom.* **22**, 2061–2069 (2011)
- Wissdorf, W., Lorenz, M., Pöhler, T., Hönen, H., Benter, T.: Atmospheric pressure ion source development: experimental validation of simulated ion trajectories within complex flow and electrical fields. *J. Am. Soc. Mass Spectrom.* **24**, 1456–1466 (2013)
- Anichich, V.: An Index of the Literature for Bimolecular Gas Phase Cation-Molecule Reaction Kinetics. Jet Propulsion Laboratory, National Aeronautics and Space Administration (2003)
- Razouk, R.I., Salem, A.S.: The adsorption of water vapor on glass surfaces. *J. Phys. Chem.* **52**, 1208–1227 (1948)
- Kochsiek, M.: Measurement of water adsorption layers on metal surfaces. *Metrologia*. **18**, 153–159 (1982)
- Lorenz, M., Schiewek, R., Brockmann, K.J., Schmitz, O.J., Gäb, S., Benter, T.: The distribution of ion acceptance in atmospheric pressure ion sources: spatially resolved APLI measurements. *J. Am. Soc. Mass Spectrom.* **19**, 400–410 (2008)
- Wißdorf, W., Lorenz, M.M., Brockmann, K.J., Schmitz, O.J., Gäb, S.S., Benter, T.: Determination of the distribution of ion acceptance (DIA) of atmospheric pressure ionization sources. In: Proceedings of the 55th ASMS Conference on Mass Spectrometry and Allied Topics. Indianapolis, IN, USA (2007)
- Constapel, M., Schellenträger, M., Schmitz, O.J., Gäb, S., Brockmann, K.J., Giese, R., Benter, T.: Atmospheric-pressure laser ionization: a novel ionization method for liquid chromatography/mass spectrometry. *Rapid Commun. Mass Spectrom.* **19**, 326–336 (2005)
- Lorenz, M., Schiewek, R., Brockmann, K.J., Mangas Suarez, A.L., Gäb, S., Schmitz, O.J., Benter, T.: Investigations of ionization mechanisms present in atmospheric pressure ion sources using APLI. In: Proceedings of the 55th ASMS Conference on Mass Spectrometry and Allied Topics. Indianapolis, IN, USA (2007)
- Brockmann, K.J., Lorenz, M., Schiewek, R., Constapel, M., Schellenträger, M., Mangas Suárez, A., Schmitz, O.J., Gäb, S., Benter, T.: Determination of the dynamic ion acceptance volume in atmospheric pressure ionization sources using APLI. In: Proceedings of the 54th ASMS Conference on Mass Spectrometry and Allied Topics. Seattle, WA, USA (2006)
- Lorenz, M., Wißdorf, W., Klee, S., Kersten, H., Brockmann, K.J., Benter, T.: Spatially and temporally resolved atmospheric pressure laser ionization as a powerful tool for the characterization of ion sources: an overview. In: Proceedings of the 58th ASMS Conference on Mass Spectrometry and Allied Topics. Salt Lake City, UT, USA (2010)
- Lorenz, M., Klee, S., Mönnikes, R., Mangas Suarez, A.L., Brockmann, K.J., Schmitz, O.J., Gäb, S., Benter, T.: Atmospheric pressure laser ionization (APLI): investigations on ion transport in atmospheric pressure ion sources. In: Proceedings of the 56th ASMS Conference on Mass Spectrometry and Allied Topics. Denver, CO, USA (2008)
- Lorenz, M., Brockmann, K.J., Wissdorf, W., Klink, D., Schmitz, O.J., Benter, T.: Distribution of ion acceptance in a fluid-dynamically optimized multi-purpose ion source. In: Proceedings of the 59th ASMS Conference on Mass Spectrometry and Allied Topics. Denver, CO, USA (2011)
- Wißdorf, W., Lorenz, M., Benter, T.: Numerical simulation of the distribution of ion acceptance (DIA) in a commercial API source. In: Proceedings of the 59th ASMS Conference on Mass Spectrometry and Allied Topics. Denver, CO, USA (2011)
- Zhou, S., Edwards, A.G., Cook, K.D., Van Berkel, G.J.: Investigation of the electrospray plume by laser-induced fluorescence spectroscopy. *Anal. Chem.* **71**, 769–776 (1999)
- Stindt, A., Warschat, C., Bierstedt, A., Panne, U., Riedel, J.: Characterisation of an inexpensive sonic spray ionisation source using laser-induced fluorescence imaging and mass spectrometry. *Eur. J. Mass Spectrom.* **20**, 21–29 (2014)
- Zhou, S., Cook, K.D.: Probing solvent fractionation in electrospray droplets with laser-induced fluorescence of a solvatochromic dye. *Anal. Chem.* **72**, 963–969 (2000)
- Girod, M., Dagany, X., Antoine, R., Dugourd, P.: Relation between charge state distributions of peptide anions and pH changes in the electrospray plume. A mass spectrometry and optical spectroscopy investigation. *Int. J. Mass Spectrom.* **308**, 41–48 (2011)
- Westerweel, J.: Fundamentals of digital particle image velocimetry. *Meas. Sci. Technol.* **8**, 1379–1392 (1997)
- Davies, T.P.: Schlieren photography—short bibliography and review. *Opt. Laser Technol.* **13**, 37–42 (1981)
- Venkatakrishnan, L., Meier, G.E.a.: Density measurements using the background oriented Schlieren technique. *Exp. Fluids*. **37**, 237–247 (2004)
- Pfeuffer, K.P., Shelley, J.T., Ray, S.J., Hietje, G.M.: Visualization of mass transport and heat transfer in the FAPA ambient ionization source. *J. Anal. At. Spectrom.* **28**, 379–387 (2013)
- Curtis, M., Keelor, J.D., Jones, C.M., Pittman, J.J., Jones, P.R., Sparkman, O.D., Fernández, F.M.: Schlieren visualization of fluid dynamics effects in direct analysis in real time mass spectrometry. *Rapid Commun. Mass Spectrom.* **29**, 431–439 (2015)
- Schiewek, R., Lorenz, M., Giese, R., Brockmann, K., Benter, T., Gäb, S., Schmitz, O.J.: Development of a multipurpose ion source for LC-MS and GC-API MS. *Anal. Bioanal. Chem.* **392**, 87–96 (2008)
- Benter, T.: Atmospheric pressure laser ionization MS. In: Gross, M., Caprioli, R.M. (eds.) *The Encyclopedia of Mass Spectrometry Volume 6: Molecular Ionization Methods*. Elsevier Science, Oxford (2007)
- Dahl, D.A.: SIMION for the personal computer in reflection. *Int. J. Mass Spectrom.* **200**, 3–25 (2000)
- Appelhans, A.D., Dahl, D.A.: SIMION ion optics simulations at atmospheric pressure. *Int. J. Mass Spectrom.* **244**, 1–14 (2005)
- Dahl, D.A., McJunkin, T.R., Scott, J.R.: Comparison of ion trajectories in vacuum and viscous environments using SIMION: insights for instrument design. *Int. J. Mass Spectrom.* **266**, 156–165 (2007)
- Pöhler, T., Kunte, R., Hoenen, H., Jeschke, P., Benter, T.: Computational fluid dynamic model of a commercial atmospheric pressure ion source. In: Proceedings of the 59th ASMS Conference on Mass Spectrometry and Allied Topics. Denver, CO, USA (2011)
- Wissdorf, W., Seifert, L., Derpmann, V., Klee, S., Vautz, W., Benter, T.: Monte Carlo simulation of ion trajectories of reacting chemical systems: mobility of small water clusters in ion mobility spectrometry. *J. Am. Soc. Mass Spectrom.* **24**, 632–641 (2013)
- Klee, S., Derpmann, V., Wißdorf, W., Klopotoski, S., Kersten, H., Brockmann, K.J., Benter, T., Albrecht, S., Bruins, A.P., Dousty, F., Kauppila, T.J., Kostianen, R., O'Brien, R., Robb, D.B., Syage, J.A.: Are clusters important in understanding the mechanisms in atmospheric pressure ionization? Part 1: reagent ion generation and chemical control of ion populations. *J. Am. Soc. Mass Spectrom.* **25**, 1310–1321 (2014)
- Klee, S., Albrecht, S., Derpmann, V., Kersten, H., Benter, T.: Generation of ion-bound solvent clusters as reactant ions in dopant-assisted APPI and APLI. *Anal. Bioanal. Chem.* **405**, 6933–6951 (2013)
- Schmitt-Kopplin, P., Englmann, M., Rossello-Mora, R., Schiewek, R., Brockmann, K.J., Benter, T., Schmitz, O.J.: Combining chip-ESI with APLI (cESILI) as a multimode source for analysis of complex mixtures with ultrahigh-resolution mass spectrometry. *Anal. Bioanal. Chem.* **391**, 2803–2809 (2008)